

## BROAD-BAND X-RAY TELESCOPE SPECTROSCOPY OF $\zeta$ PUPPIS

M. F. CORCORAN,<sup>1</sup> J. H. SWANK, P. J. SERLEMITOS, E. BOLDT, R. PETRE, F. E. MARSHALL, K. JAHODA,  
 R. MUSHOTZKY, A. SZYMKOWIAK, K. ARNAUD,<sup>2</sup> A. P. SMALE,<sup>1</sup> K. WEAVER,<sup>2</sup> AND S. S. HOLT

Laboratory for High-Energy Astrophysics, NASA/Goddard Space Flight Center, Greenbelt, MD 20771

Received 1992 December 14; accepted 1993 February 5

### ABSTRACT

The Broad-Band X-Ray Telescope (BBXRT) obtained moderate-resolution ( $\sim 90$  eV) X-ray spectra of the O4 f star  $\zeta$  Pup during the STS 35/Astro 1 mission in 1990 December. Despite the shortness of the observation (600 s), the data show a surprising amount of detail. We report the detection of an O absorption edge produced by ionized overlying wind material and K-shell line emission from Mg produced by a thermal plasma of temperature near  $6 \times 10^6$  K. The data are used to place constraints on the location, temperature, and amount of the X-ray-emitting gas, as well as the abundance and ionization of the wind material.

*Subject headings:* stars: early-type — stars: individual ( $\zeta$  Puppis) — stars: mass loss — X-rays: stars

### 1. INTRODUCTION

X-ray spectroscopy provides a useful probe of the dynamics and composition of stellar winds from massive stars. Because the source of the X-radiation is buried within the stellar wind whose density varies outwardly as  $r^{-2}$ , the amount of X-ray absorption gives a direct measure of the distance of the X-ray-emitting gas above the stellar surface. Emission lines and/or absorption edges can serve to trace the chemical and ionic abundance in the wind. The X-ray spectrum can be used to identify and define the physical mechanism that produces the observed X-ray emission and gives direct evidence of the stability and nature of the extended outer atmospheres of hot stars.

X-ray emission does not merely serve as a passive probe of stellar winds, however; the X-ray flux has a direct influence on the ion balance since X-rays can increase the ionization of the wind through Auger ionization (Cassinelli & Olson 1979). Observations of O VI and other “superionized” lines in the UV spectra of many O stars (Rogerson & Lamers 1975) have suggested the importance of this effect. Quantitative modeling is lacking, due to a lack of accurate knowledge of the physical properties of the X-ray source.

The flight of the Broad-Band X-Ray Telescope (BBXRT) in 1990 December offered an unprecedented opportunity to increase our knowledge of the properties of X-ray emission from massive stars. During its maiden flight, BBXRT observed three hot stars:  $\zeta$  Pup, EZ CMa, and  $\zeta$  Ori. Despite some technical problems with the instrument pointing assembly and a weather-shortened mission which drastically curtailed integration times for each of these stars (by as much as a factor of 10), the data obtained were of comparable quality to those obtained with far longer exposures on similar stars by the *Einstein* Solid State Spectrometer (SSS). In this paper we report our observation of  $\zeta$  Pup with BBXRT. The spectrum we obtained, though underexposed, shows a surprising amount of detail, such as the presence of an absorption edge due to ionized oxygen, and a well-resolved emission complex produced by a blend of Mg K shell emission at 1.3 keV. We use the

spectrum to determine a well-constrained source temperature, to put limits on the location and amount of X-ray-emitting material, and to probe the chemical and ionic abundance of the wind.

### 2. THE OBSERVATION

BBXRT (Serlemitsos et al. 1992) consisted of two co-aligned X-ray telescopes (the “A” telescope and the “B” telescope), each containing an X-ray mirror + solid-state X-ray detector. The mirrors were composed of nested gold-coated, thin aluminum conical foils which design offers the advantage of high throughput over a wide range of X-ray energies (0.3–12 keV) with good ( $\sim 90$  eV) spectral resolution, while providing arcminute-scale spatial resolution. The detectors were cooled Li-drifted silicon detectors similar to those employed by the *Einstein* SSS, but with better energy resolution (by about a factor of 2) and lower internal background (by about a factor of 100). Each detector was segmented into five regions or “pixels” so as to provide a coarse imaging capability. The central or zeroth pixel was a circle of about 4' diameter; the four outer pixels extended coverage to the full 17' diameter field.

BBXRT observed  $\zeta$  Pup once during the 9 day mission for only 600 s for a total of about 600 source counts. The observation was made entirely during orbit night so contamination by airglow was minimized. The BBXRT A and B detector fields of view superposed on an IPC map of the  $\zeta$  Pup region are shown in Figure 1. Uncertainties in the pointing system caused the observation to be made about 5.1 off-axis and as a result  $\zeta$  Pup was detected in outer pixels in both telescopes (pixels A3 and B1). Pointing problems also caused a significant amount of stellar flux to be intercepted by the mask which separated the pixels or to be scattered out of the detector field of view. Ray-tracing indicates that about 7.4% of the flux was intercepted by the mask while 8.1% of the flux was scattered out of the field of view. Table 1 lists details of the observation and gives the nominal counting rate in an off-source pixel as an upper limit to the background for each detector. These values are upper limits to the background due to scattering of source counts into the off-source pixels. Figure 2 shows the counting rate in the two on-source and two off-source pixels during the observation.

<sup>1</sup> Also Universities Space Research Association, Goddard Space Flight Center, Greenbelt MD 20771.

<sup>2</sup> Also Astronomy Program, University of Maryland, College Park, MD 20742.

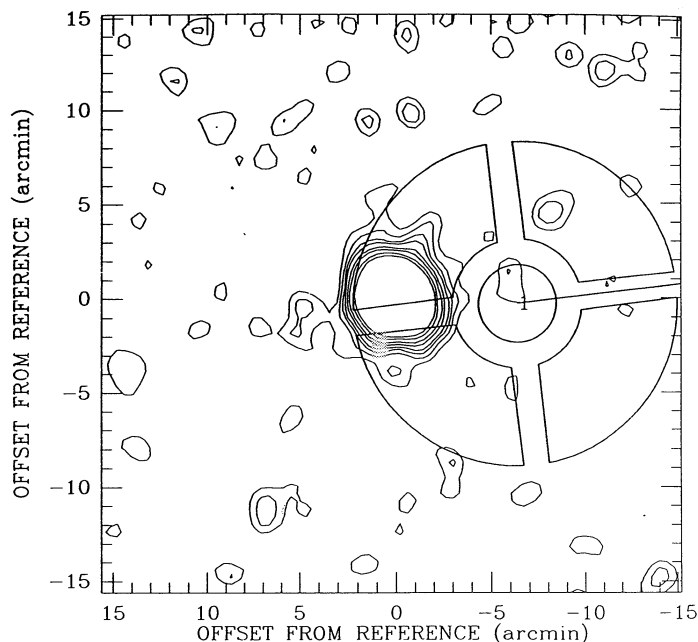


FIG. 1a

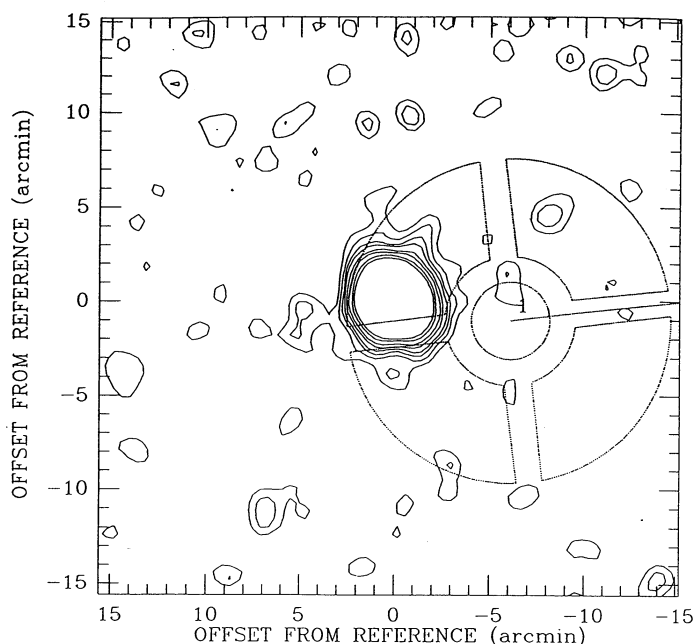


FIG. 1b

FIG. 1.—Field-of-view of the BBXRT A and B detectors superposed on an *Einstein* IPC image (sequence 5110) of the  $\zeta$  Pup region.  $\zeta$  Pup is the strong source in the center of the field. (a) A detector; (b) B detector. A line marks the A1/A2 (B3/B4) border for the A (B) detector. Numbering of the outer pixels increases in the anticlockwise (clockwise) direction for the A (B) detector.

### 3. ANALYSIS

Though  $\zeta$  Pup was primarily observed in pixels A3 and B1, in order to conserve source photons which were scattered into surrounding pixels we co-added data from the 5 pixels for each telescope. We binned the co-added spectra so as to have greater than 10 counts in each spectral bin. We estimated background for the observation by co-adding observations of night-time blank sky which were accumulated during the mission. After subtracting background, we analyzed the binned co-added spectra simultaneously using a response matrix appropriate for detector A3 and detector B1 corrected for vignetting of the 5:1 off-axis source (Weaver et al. 1992). We ignored channels below about 0.5 keV and above about 2.5 keV where background contamination dominates. We modeled the data using a Raymond-Smith thermal spectrum (Raymond 1991) with interstellar absorption (Morrison & McCammon 1983) fixed at  $N_H = 10^{20} \text{ cm}^{-2}$  (Chlebowski, Harnden, & Sciortino 1989). Opacity of the ionized stellar wind is dominated by CNO K-shell absorption (Cassinelli & Olson 1979), so we included an O absorption edge in the model

as an approximation of the stellar wind opacity in the usable spectral range ( $E > 0.5 \text{ keV}$ ), with optical depth of the edge ( $\tau_0$ ) and edge energy ( $E_{\text{edge}}$ ) as free parameters. We found that one

Parameter	Value
Start (MET) <sup>a</sup>	5 <sup>d</sup> 23 <sup>h</sup> 16 <sup>m</sup> 22 <sup>s</sup>
Exposure (s)	604
Pixel A3 rate <sup>b</sup> (counts s <sup>-1</sup> )	0.63 ± 0.03
Pixel B1 rate <sup>b</sup> (counts s <sup>-1</sup> )	0.52 ± 0.03
Pixel A1 rate <sup>b</sup> (counts s <sup>-1</sup> )	0.06 ± 0.03
Pixel B3 rate <sup>b</sup> (counts s <sup>-1</sup> )	0.13 ± 0.04
Off-axis distance (°)	5.1

<sup>a</sup> MET 0<sup>d</sup>00<sup>h</sup>00<sup>m</sup>00<sup>s</sup> = 1991 Dec 2 06:30 UT.

<sup>b</sup> Rates in channels 41–512 (0.6–12 keV).

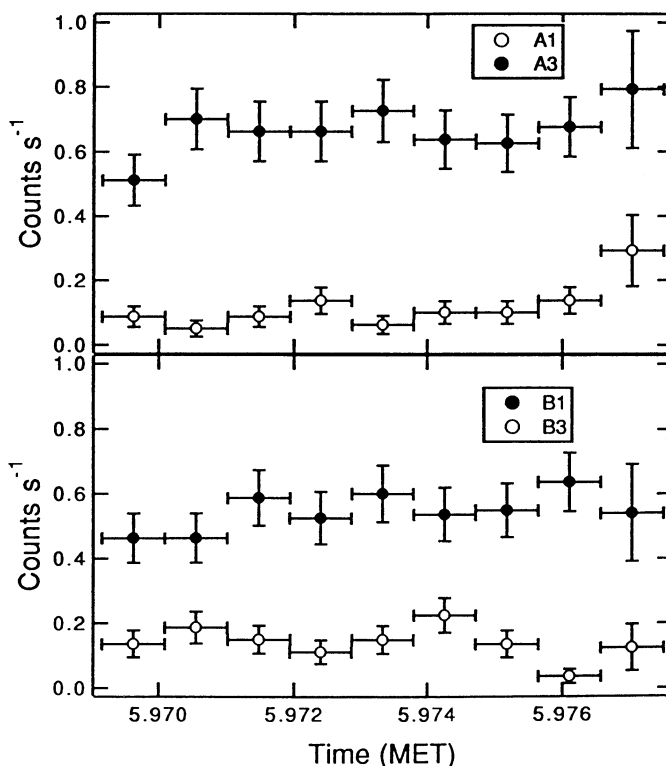


FIG. 2.—Counting rates in source pixels A3 and B1 (filled circles) and in two off source pixels (A1 and B3, open circles) during the observation of  $\zeta$  Pup.

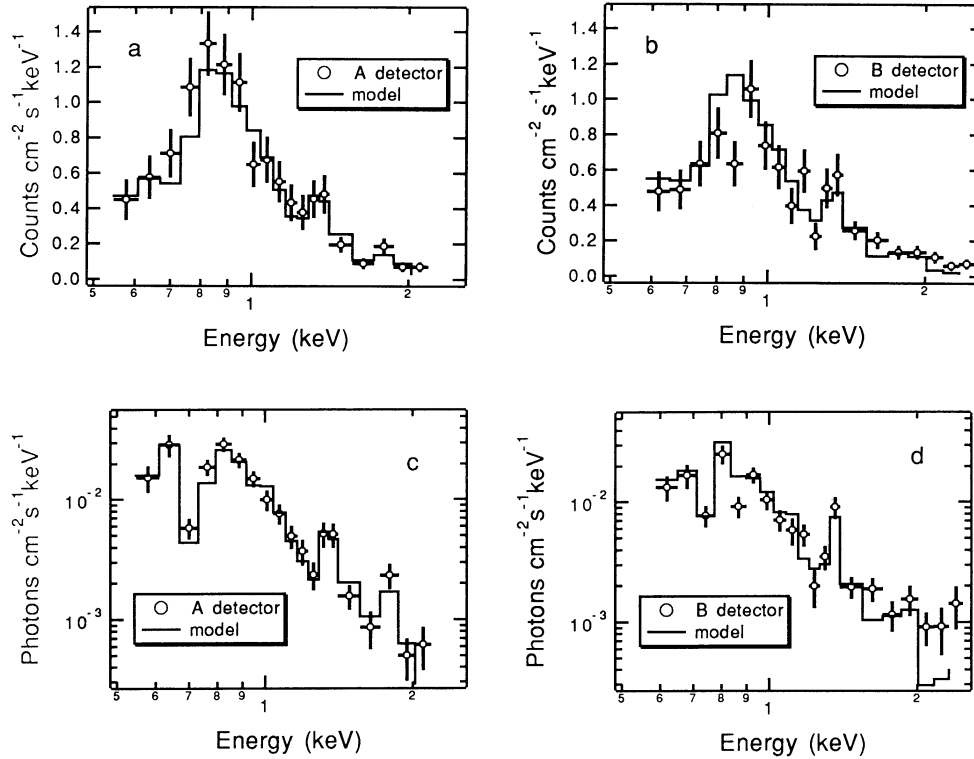


FIG. 3.—BBXRT spectra of  $\zeta$  Pup. (a) Observed spectrum derived from co-addition of A detector pixels + best fit model (as described in the text) folded through the A detector response; (b) observed spectrum derived from co-addition of B detector pixels + best fit model folded through the B detector response; (c) best-fit model + unfolded A detector spectrum; (d) best fit model + unfolded B detector spectrum. The low channel at 0.9 keV in the B detector spectrum was ignored during the model fitting.

channel in the B detector spectrum near 0.9 keV dominated the contribution to  $\chi^2$ , so we ignored this channel when fitting. Table 2 gives the parameters of our best fit to the co-added spectra. Figure 3 compares the model with the data.

#### 4. DISCUSSION

##### 4.1. Characteristics of the X-Ray Emission

###### 4.1.1. The Location of the X-Ray Plasma

Our determination of significant local absorption for  $\zeta$  Pup adds to a growing list of evidence suggesting the importance of local absorption in interpreting X-ray spectra from hot stars. Cassinelli & Swank (1983) have published moderate-resolution SSS observations of the Orion supergiants, and while they do not report the existence of any absorption edges in their SSS

spectra, they typically find absorbing columns which are significantly larger than interstellar. Waldron (1991) has recently shown a direct correlation between X-ray hardness ratio and 6 cm radio emission for a sample of hot stars, which he interpreted in terms of stellar wind absorption. In addition, recent *ROSAT* observations of  $\zeta$  Pup (Schmitt 1992) suggest the presence of local absorption.

The detection of local absorption is important since it means we can use the amount of absorbing material to determine the location of the X-ray-emitting material along the line of sight. We have that

$$\tau_{ij} = \int_{r_0}^{\infty} \sigma_{ij} n_{ij}(r) dr, \quad (1)$$

where  $\tau_{ij}$  is the optical depth of the edge produced by element  $i$  in the  $j$ th stage of ionization,  $\sigma_{ij}$  the absorption cross section,  $n_{ij}(r)$  the number density of the ion in the wind at a distance  $r$  from the center of the star, and  $r_0$  the distance from the center of the star to the X-ray-emitting plasma. We can rewrite equation (1) as

$$\tau_{ij} = A_i f_{ij} \sigma_{ij} \int_{r_0}^{\infty} n_w \frac{n_H}{n_w} dr, \quad (2)$$

where  $A_i$  is the number density of the element relative to hydrogen,  $f_{ij}$  is the ion fraction,  $n_w$  is the number density in the wind and  $n_H/n_w$  the fractional number density of hydrogen in the wind. We have

$$n_w(r) = \frac{\dot{M}}{4\pi\mu m_H r^2 V_{\infty} (1 - R/r)^{\beta}}, \quad (3)$$

where  $\dot{M}$  is the mass-loss rate,  $\mu$  is the mean atomic weight of

TABLE 2

BEST FIT TO CO-ADDED NET SPECTRUM

Parameter	Value <sup>a</sup>
$\log T$ (K) .....	6.85 (+0.04; -0.05)
$\log EM$ ( $\text{cm}^{-3}$ ) <sup>b</sup> .....	55.73 (+0.14; -0.14)
$\log f_x$ ( $\text{ergs cm}^{-2} \text{s}^{-1}$ ) <sup>b,c</sup> .....	-10.37 (+0.13; -0.01)
$\tau_0$ .....	2.32 (+1.23; -1.28)
$E_{\text{edge}}$ (keV) .....	0.66 (+0.06; -0.01)
Mg/Mg <sub>⊙</sub> .....	2.00 (+1.32; -0.74)
Fe/Fe <sub>⊙</sub> .....	0.65 (+0.66; -0.35)
$\chi^2_r$ .....	1.3

<sup>a</sup> Errors are 1  $\sigma$  confidence limits.

<sup>b</sup> Corrected for loss of photons by scattering.

<sup>c</sup> Flux in 0.4–2.0 keV band corrected for ISM + wind absorption.

wind material,  $R$  is the radius of the star, and  $\beta$  the wind acceleration parameter which is generally close to 1 (Groenewegen & Lamers 1989).

For  $\zeta$  Pup,  $\dot{M} \approx 4.7 \times 10^{-6} M_{\odot} \text{ yr}^{-1}$ ,  $V_{\infty} = 2660 \text{ km s}^{-1}$  (Chlebowski & Garmany 1991) and  $R = 20 R_{\odot}$ . We take  $\beta = 1$  for simplicity. Although there is some evidence for abundance enhancements in  $\zeta$  Pup (Conti & Frost 1977; Kudritzki, Simon, & Puls 1982, § 4.2.1) we will not appreciably bias our results if we fix the abundance of O at the solar value. Assuming solar abundances, we have that  $\mu \approx 1.26$ ,  $n_{\text{H}}/n_{\text{w}} = 0.93$  and  $A_i = 6.61 \times 10^{-4}$ . Calculations by Drew (1989) suggest that most of the oxygen in winds from stars like  $\zeta$  Pup is in the form of O IV, result which is not inconsistent with our measurement of the edge energy (§ 4.2.2). Assuming that all O is in the form of O IV, we have that  $f_{ij} = 1.0$ ,  $\sigma_{ij} = 0.496 \times 10^{-18} \text{ cm}^2$  (Daltabuit & Cox 1972) and  $\tau_{ij} = \tau_{\text{O}} = 2.32$ . Solving equation (3) for  $r_0$  we find

$$r_0 = \frac{R}{1 - \exp(-0.108\tau_{ij})}. \quad (4)$$

With  $\tau_{ij} = 2.32$  we find that  $r_0 = 4.5$ , that is, that the hot plasma is located about 3.5 stellar radii above the surface of the star. The 90% confidence limits on  $\tau_{ij}$  ( $1.0 < \tau_{ij} < 3.5$ ) suggest that the bulk of the X-ray plasma is confined to the range  $3.1 < r_0/R < 9.7$ .

#### 4.1.2. X-Ray Flux

Pointing problems caused a fraction of the stellar flux to fall onto the interpixel mask or outside of the field of view (FOV). Ray-tracing suggests that scattering onto the mask or out of the FOV removed about 15.5% of the flux from the beam. Taking the loss due to scattering into account, and with an assumed distance to  $\zeta$  Pup of 450 pc, we find that  $\log \text{EM} \approx 55.73$ . This can be compared to the total wind emission measure, defined as

$$\text{EM}(\text{wind}) = \int n_{\text{w}}^2 dV \text{ cm}^{-3}. \quad (5)$$

With  $n_{\text{w}}(r)$  given above, and integrating outward from just above the stellar photosphere ( $r = 1.01R$ ), we find that the total emission measure of the wind is  $\log \text{EM}(\text{wind}) \approx 59.9$ . Thus the hot X-ray plasma represents only  $10^{-5}$  or so of the total wind material. The observed to total wind emission measure ratio we find is similar to ratios reported elsewhere for other hot stars with large mass-loss rates (Cassinelli et al. 1981; Cassinelli & Swank 1983). This suggests that only a very small amount of the available wind material is actually heated to X-ray-producing temperatures.

After correcting for scattering, the observed X-ray flux (uncorrected for absorption) in the *Einstein* bandpass (0.4–4.5 keV) is  $f_{\text{X}} = 2.1 \times 10^{-11} \text{ ergs cm}^{-2} \text{ s}^{-1}$ . This is about a factor of 2 higher than the value of  $f_{\text{X}} = 1.1 \times 10^{-11} \text{ ergs cm}^{-2} \text{ s}^{-1}$  derived by analysis of the IPC spectrum by Cassinelli et al. (1981). This discrepancy may be evidence of intrinsic variability. IPC observations suggest that the X-ray flux from some OB stars does vary by as much as a factor of 2 (Snow et al. 1981; Collura et al. 1989). However, Snow et al. found no evidence of intrinsic variability in the case of  $\zeta$  Pup. Collura et al. (1989) reanalyzed the IPC observations and concluded that the X-ray emission from  $\zeta$  Pup was variable, but Harnden (1993) suggests that the variability reported by Collura et al. is probably the result of a gain variation which was uncorrected in the REV1 IPC data. The intrinsic source luminosity is

highly dependent upon the amount of local absorption. Correcting the observed flux for interstellar plus local absorption using our best-fit value of the oxygen edge optical depth, we find that  $L_{\text{X}} = 1.0 \times 10^{33} \text{ ergs s}^{-1}$  in the IPC bandpass. This implies that the  $L_{\text{X}}/L_{\text{bol}}$  ratio in the IPC bandpass for our observation of  $\zeta$  Pup is

$$-\log \frac{L_{\text{X}}}{L_{\text{bol}}} = 6.48 \pm 0.05 \quad (6)$$

(using  $L_{\text{bol}} = 3.0 \times 10^{39} \text{ ergs s}^{-1}$  as given by Cassinelli et al.). Our  $L_{\text{X}}/L_{\text{bol}}$  ratio is at least a factor of 3 larger than that reported by Cassinelli et al. ( $-\log L_{\text{X}}/L_{\text{bol}} = 7.07$ ) and by Chlebowski et al. ( $-\log L_{\text{X}}/L_{\text{bol}} = 7.00$ ) due in part to our determination of and correction for local absorption.

### 4.2. X-Rays as a Probe of the Stellar Wind

#### 4.2.1. Chemical Abundance

In addition to establishing the thermal nature of the X-ray emission, the presence of emission lines in the X-ray spectrum also allows us to examine the chemical abundance of a limited number of elements in the outer atmosphere of  $\zeta$  Pup. This is important since previous analyses of the He spectrum in the visible band suggest that He is enhanced in  $\zeta$  Pup. The exact value of the He enhancement is uncertain, with published values of 30% (Conti & Frost 1977; Kudritzki et al. 1983) up to 100% (Voels 1989). The significance of the photospheric abundance determinations is unclear since, as Conti (1988) pointed out, determination of abundances for hot stars from analysis of photospheric spectra is difficult due to uncertainties in the model atmosphere codes.

Unfortunately, we cannot derive an independent measure of the He abundance from analysis of the X-ray spectrum since the BBXRT spectrum is fairly insensitive to the amount of He in the X-ray-emitting gas. We therefore modeled the spectrum with the He abundance allowed to float between the solar value and twice the solar value and found that the preferred model had He at twice the solar abundance. However, changing the He abundance to any value in the range did not significantly degrade the fit, nor substantially change the values of the fit parameters we derived.

The X-ray spectrum provides a much better diagnostic of the atmospheric Mg abundance, due to the presence of the strong Mg XI K-shell line at about 1.3 keV. In order to match the observed strength of the Mg line, we needed to increase the Mg abundance to twice the solar abundance. The X-ray spectrum is also somewhat sensitive to the abundance of Fe due to a blend of Fe XVII–Fe XVIII L-shell emission near 0.9 keV. Our best-fit value shows that Fe is underabundant by about 65% relative to the solar value. The spectrum in this region is complicated by the presence of Ne K-shell emission at 0.92 keV, and as a result we cannot use the spectrum to put very stringent constraints on the Fe abundance; we cannot rule out a solar (or even above-solar) Fe abundance.

#### 4.2.2. Oxygen Ionization

The presence of local absorption is also important since our determination of the energy of the O absorption edge determines (in principle) the dominant ionization stage of O in the wind material between the X-ray plasma and the observer. For neutral oxygen the edge is at 0.53 keV, while for O VI the edge occurs at 0.67 keV (Daltabuit & Cox 1972). Unfortunately, the limited energy resolution of BBXRT and the fact that the spectrum was so severely underexposed do not allow us to strongly



constrain the energy of the O edge. Our 90% confidence limits on the energy of the O edge are  $0.65 < E_{\text{edge}} < 0.72$ , which is sufficient to constrain (at the  $1\sigma$  confidence level) the dominant ionization stage of O as O v or less. This is consistent with the work of Drew (1989) who found O iv to be the dominant stage of oxygen ionization for hot stars having photospheric temperatures near the  $\zeta$  Pup value ( $\sim 40,000$  K).

## 5. CONCLUSIONS

Our BBXRT observation of  $\zeta$  Pup confirms the thermal nature of the X-ray emission and suggests that the X-rays come from a relatively small amount of hot gas buried within the ionized stellar wind. Similar X-ray observations of hot stars by the SSS have suggested the presence of multiple-temperature components (Swank 1985) or high-energy tails (Chen & White 1991). Unfortunately, our BBXRT spectrum was too underexposed to address these issues.

As yet there is no detailed mechanism to explain how and where O stars produce X-rays. Our determination that at least some of the X-ray-emitting gas lies about 4 stellar radii above the photosphere seemingly rules out the thin coronal model (Cassinelli & Olson 1979; Waldron 1984) in which the X-rays are produced in a thin region just above the photosphere. However, we cannot rule out the possibility that some X-rays are produced closer to (or farther from) the star than 4 stellar radii above the photosphere. In particular, the X-ray-emitting region could be much closer to the stellar photosphere than 4 stellar radii if the ion balance for oxygen in the wind is shifted

away from  $\text{O}^{+3}$ . An alternative to the coronal model suggests that X-rays are produced by shocks which result from radiative instabilities in the wind flow (Lucy & White 1980; Owocki, Castor, & Rybicki 1988). If we interpret the X-ray emission as coming from shocked gas, then the temperature of the X-ray emission,  $T \sim 7 \times 10^6$  K, implies a shock jump velocity of about  $500 \text{ km s}^{-1}$  in the comoving frame. A velocity of a few hundred  $\text{km s}^{-1}$  agrees fairly well with the magnitude of turbulent wind velocities as deduced from analysis of the UV P Cygni features for many hot stars (Prinja & Howarth 1986).

We also point out that detailed knowledge of the X-ray spectrum can be used to determine such fundamental quantities as abundances and ion balances, information which is often difficult to deduce by other means such as fine analysis of the photospheric or wind spectrum. Finally, it is important to note that knowledge of the intrinsic stellar X-ray luminosity is predicated upon accurate knowledge of both interstellar and circumstellar absorption. In the case of  $\zeta$  Pup, the correction for wind absorption increases the intrinsic  $L_X/L_{\text{bol}}$  ratio in the IPC band by at least a factor of 2.

We would like to thank Wayne Waldron and Rick Harnden for a careful reading of the manuscript and for helpful comments. This work was conducted when MFC was a National Research Council Resident Research Associate at the Goddard Space Flight Center; this support is gratefully acknowledged.

## REFERENCES

- Cassinelli, J., & Olson, G. 1979, *ApJ*, 229, 304  
 Cassinelli, J. P. & Swank, J. H., 1983, *ApJ*, 271, 681  
 Cassinelli, J. P., et al. 1981, *ApJ*, 250, 677  
 Chen, W., & White, R. L. 1991, *ApJ*, 366, 512  
 Chlebowski, T., & Garmany, C. D. 1991, *ApJ*, 368, 241  
 Chlebowski, T., Harnden, F. R., Jr., & Sciortino, S. 1989, *ApJ*, 341, 427  
 Collura, A., Sciortino, S., Serio, S., Vaiana, G. S., Harnden, F. R., Jr., & Rosner, R. 1989, *ApJ*, 338, 296  
 Conti, P. S. 1988, in *O Stars and Wolf-Rayet Stars*, ed. P. S. Conti & A. B. Underhill (NASA SP-497), 134  
 Conti, P., & Frost, S. A. 1977, *ApJ*, 212, 728  
 Daltabuit, E., & Cox, D. E. 1972, *ApJ*, 177, 855  
 Drew, J. E. 1989, *ApJS*, 71, 267  
 Groenewegen, M. A. T., & Lamers, H. 1989, *A&AS*, 79, 359  
 Harnden, F. R., Jr., 1993, private communication  
 Kudritzki, R. P., Simon, K. P., & Puls, J. 1987, *A&A*, 173, 293  
 Kudritzki, R. P., Simon, K. P., & Hamann, W.-R. 1983, *A&A*, 118, 245  
 Lucy, L. B., & White, R. L. 1980, *ApJ*, 241, 300  
 Morrison, R., & McCammon, D. 1983, *ApJ*, 270, 119  
 Owocki, S. P., Castor, J. I., & Rybicki, G. B. 1988, *ApJ*, 335, 914  
 Prinja, R. K., & Howarth, I. D. 1986, *ApJS*, 61, 357  
 Raymond, J. 1991, private communication  
 Rogerson, J. E., & Lamers, H. 1975, *Nature*, 256, 190  
 Schmitt, J. H. 1992, private communication  
 Serlemitsos, P. J., et al. 1992, in *Frontiers of X-Ray Astronomy*, ed. Y. Tanaka & K. Koyama (Frontiers Science Series-2), 221  
 Snow, T. P., Cash, W., & Grady, C. A. 1981, *ApJ*, 244, L19  
 Swank, J. H. 1985, in *The Origin of Nonthermal Heating/Momentum in Hot Stars*, ed. A. B. Underhill & A. G. Michalitsianos (NASA Publ. 2358), 86.  
 Voels, S. A. 1989, Ph.D. thesis, Univ. Colorado, Boulder  
 Waldron, W. L. 1984, *ApJ*, 282, 256  
 ———. 1991, *ApJ*, 382, 603  
 Weaver, K. A., et al. 1992, private communication